RSC Advances

ROYAL SOCIETY OF CHEMISTRY

www.rsc.org/advances

Journal Name

RSCPublishing

COMMUNICATION

Fabrication of a novel magnetic yolk-shell Fe_3O_4@mTiO_2@mSiO_2 nanocomposite for selective enrichment of endogenous phosphopeptides from the complex sample

Cite this: DOI: 10.1039/x0xx00000x

Received 00th January 2012,
Accepted 00th January 2012

DOI: 10.1039/x0xx00000x

www.rsc.org/

Hao Wan,[ab] Jinan Li,[b] Wenguang Yu,[b] Zheyi Liu,[b] Quanqing Zhang,[b] Weibing Zhang*[a] and Hanfa Zou*[b]

The yolk-shell nanocomposite composed of a magnetic mesoporous anatase TiO_2 (Fe_3O_4@mTiO_2) core, a medium cavity and an outmost mesoporous silica (mSiO_2) shell was successfully fabricated. Combination of the strong magnetic response, improved diffusion of peptides, numerous affinity sites towards phosphopeptides and the size-exclusion effect, the nanocomposite demonstrated the high enrichment efficacy and selectivity towards endogenous phosphopeptides from human serum.

Phosphorylation is one of the most important and ubiquitous post-translational modifications. The phosphorylation of endogenous peptides is involved in lots of biological and pathological variations, which makes endogenous phosphopeptides as the potential biomarkers with high clinical sensitivity and specificity. However, due to the interference and cover of signal by high-abundance proteins and endogenous non-phosphopeptides in the complex sample, the mass spectrometry (MS) detection of endogenous phosphopeptides still remains challenging.[1]

Selective enrichment of endogenous phosphopeptides exists as an effective way to exclude the interference and improve the precision and sensitivity of MS detection. Compared with other enrichment methods, metal oxide affinity chromatography (MOAC) has been reported to demonstrate higher binding selectivity and sensitivity to phosphate group. Among these metal oxides, anatase TiO_2 has been most widely utilized for selective enrichment of phosphopeptides from various enzymatic digests due to the higher affinity and more tolerance of many biochemical reagents.[2] However, because of the occupation and cover of affinity sites on anatase TiO_2 by some large-molecule phosphoproteins and non-phosphoproteins in the complex sample, the enrichment selectivity and efficacy towards endogenous phosphopeptides would be highly affected.[3] Appearing as a molecular sieve, mesoporous SiO_2 has been applied in different systems to differentiate small and large molecules based on the size-exclusion effect.[4] But due to the low-efficiency and time-consuming centrifugation separation, the practical application of mesoporous SiO_2 in the exclusion of proteins beneficial for efficient and selective enrichment of endogenous phosphopeptides is limited. Recently, the magnetic yolk-shell structure has been attracting more and more attentions. On one hand, the magnetic response would simplify the process of sample separation. On the other hand, the cavity would be beneficial for the diffusion of guest molecules and also enhance the contact area between the substrate and guest molecules.[5] Attributed to all above unique properties, an integration of mesoporous SiO_2, anatase TiO_2 and a magnetic yolk-shell structure should better fulfil the requirement for selective enrichment of endogenous phosphopeptides from the complex sample.

Herein, for highly efficient and selective enrichment of endogenous phosphopeptides from the complex sample, we elaborately fabricated a novel magnetic yolk-shell nanocomposite (Scheme 1). Starting from Fe_3O_4 nanoparticles, we directly coated a layer of amorphous TiO_2, followed by solvothermal reaction assisted pore formation and crystallization of amorphous TiO_2 into anatase type (Fe_3O_4@mTiO_2). Subsequently, with the help of PVP the Fe_3O_4@mTiO_2 was encapsulated by a dense SiO_2 shell (Fe_3O_4@mTiO_2@nSiO_2), onto which another outmost mesoprosous

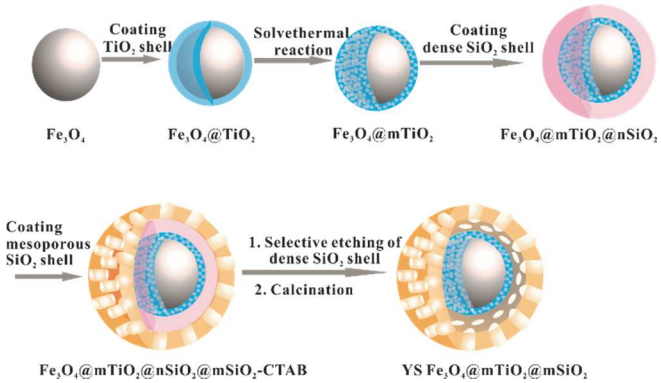

Scheme 1 The schematic illustration of the fabrication process of YS Fe_3O_4@mTiO_2@mSiO_2

SiO_2 shell was assembled by using CTAB as a structure director (Fe_3O_4@mTiO_2@nSiO_2@mSiO_2-CTAB). After the selective etching of the dense SiO_2 shell by Na_2CO_3 solution and calcination of CTAB and PVP, the final nanocomposite (YS Fe_3O_4@mTiO_2@mSiO_2) was obtained. The YS Fe_3O_4@mTiO_2@mSiO_2 was suitable for selective enrichment of endogenous phosphopeptides from the complex sample: (1) the outmost mSiO_2 shell would act as a size-dependent sieve to exclude large-molecule proteins out; (2) the medium cavity would improve the diffusion of endogenous phosphopeptides and enhance the contact area between endogenous phosphopeptides and the Fe_3O_4@mTiO_2 core; (3) the Fe_3O_4@mTiO_2 core with high surface area would not only provide numerous affinity sites to capture endogenous phosphopeptides but also simplify the process of sample separation.

Shown in Fig. 1, the diameter of as-synthesized Fe_3O_4@mTiO_2 core distributed around 200-300 nm (Fig. 1c). After encapsulation with the dense SiO_2 shell, a well-defined core-shell structure was obtained (Fig. 1d). Under the direction of CTAB, another outmost mSiO_2 shell was successfully assembled and the corresponding size increased to 500-600 nm (Fig. 1e). The yolk-shell structure appeared after the selective etching process, which was based on the unexpected differentiated dissolution behaviours, stemming from stabilization of the outmost mSiO_2 shell by CTAB (Fig. 1f).[6] Through the experiment, it was found out the mass ratio of the Fe_3O_4@mTiO_2@nSiO_2@mSiO_2-CTAB and Na_2CO_3 was an indispensable factor for the successful fabrication of the final yolk-shell structure. Fixing the amount of Na_2CO_3 at 212 mg, we varied the added amount of Fe_3O_4@mTiO_2@nSiO_2@mSiO_2-CTAB. Based on the TEM results (Fig. 2), if the added amount of Fe_3O_4@mTiO_2@nSiO_2@mSiO_2-CTAB was limited, an etching of both dense SiO_2 and outmost mSiO_2-CTAB shells happened. On the contrast, when the added amount of Fe_3O_4@mTiO_2@nSiO_2@mSiO_2-CTAB was too much, the

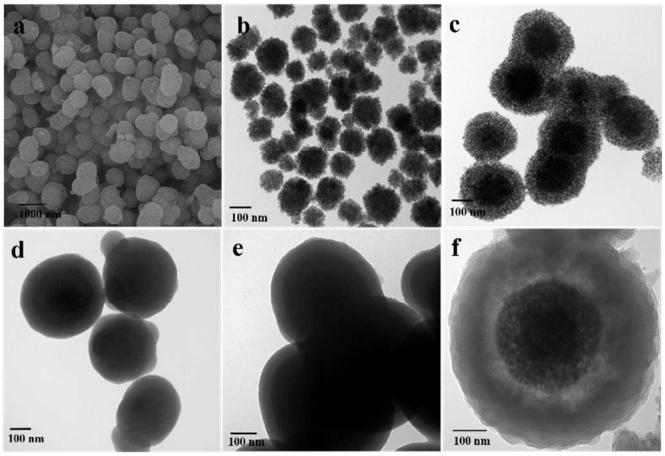

Fig 1. The SEM image of (a) YS Fe_3O_4@mTiO_2@mSiO_2; The TEM images of (b) Fe_3O_4, (c) Fe_3O_4@mTiO_2, (d) Fe_3O_4@mTiO_2@nSiO_2, (e) Fe_3O_4@mTiO_2@nSiO_2@mSiO_2-CTAB and (f) YS Fe_3O_4@mTiO_2@mSiO_2.

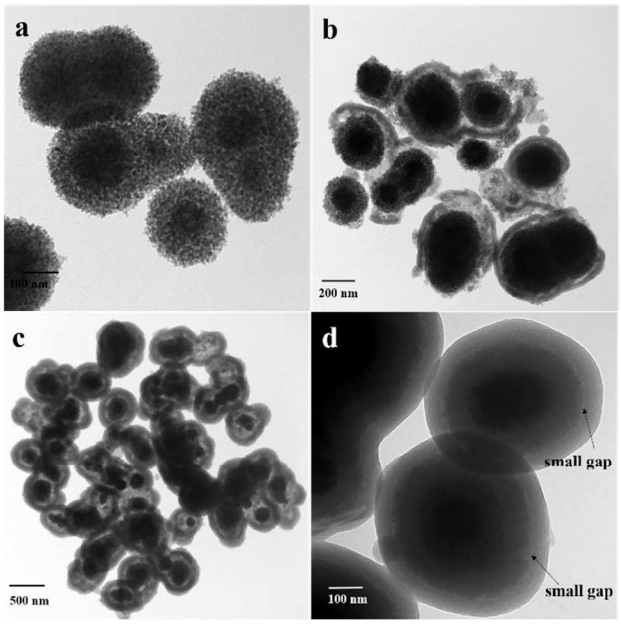

Fig. 2 TEM images of nanoparticles after the selective etching process by Na_2CO_3 solution when the added amount of Fe_3O_4@mTiO_2@nSiO_2@mSiO_2-CTAB was (a) 50 mg, (b) 100 mg, (c) 150 mg and (d) 250 mg.

Na_2CO_3 solution was not strong enough to completely etch the dense SiO_2 shell away, leaving a small gap. So only when the added amount of Fe_3O_4@mTiO_2@nSiO_2@mSiO_2-CTAB was appropriate, can a well-defined yolk-shell structure be successfully developed. According to the XRD analysis, all diffraction peaks of original magnetic nanoparticles can be perfectly indexed to the magnetite phase of Fe_3O_4 (JCPDS 19-629) and the final nanoparticles showed additional diffraction peaks of anatase TiO_2 (JCPDS 21-1272) (Fig. S1, ESI†). The EDS element mapping illustrated the exact distribution of fundamental compositions, further identifying the successful fabrication of YS Fe_3O_4@mTiO_2@mSiO_2 (Fig. 3).

Then, the N_2 adsorption experiment was used to probe the detailed structure information about YS Fe_3O_4@mTiO_2@mSiO_2. The adsorption–desorption isotherms exhibited the typical IV pattern of the mesoporous material with a distinct H3 hysteresis loop, proving the ink-bottle-type

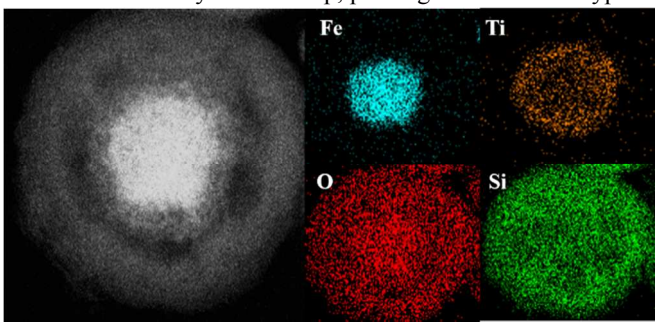

Fig. 3 The EDS element mapping of YS Fe_3O_4@mTiO_2@mSiO_2.

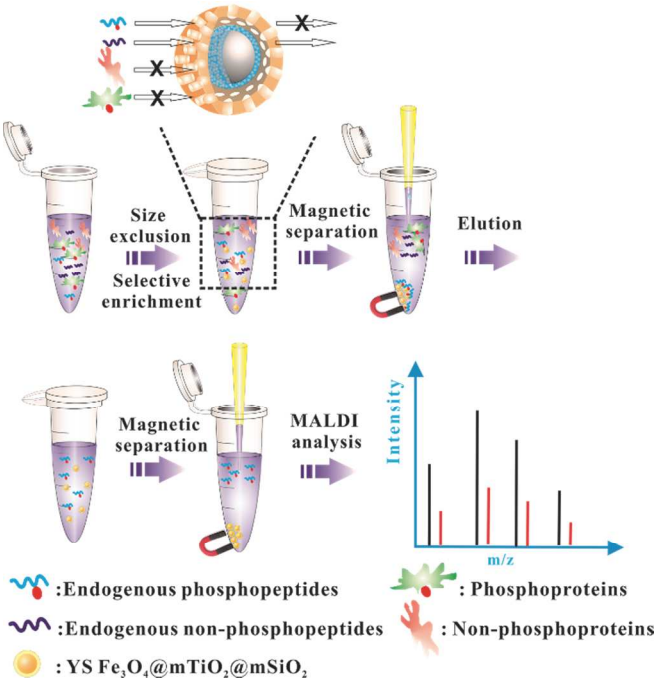

Scheme 2 The process of selective enrichment of endogenous phosphopeptides from the complex sample with YS Fe_3O_4@$mTiO_2$@$mSiO_2$.

pores in which large cavities are connected by narrow windows.[7] The pore distribution showed three main pore diameters of 2.7, 3.9 and 9.1 nm, which could be ascribed to pores distributing within the outmost $mSiO_2$ shell and inner mesoporous anatase TiO_2, respectively (Fig. S2, ESI†). Besides, the Fe_3O_4@$mTiO_2$ was also conducted through the BET and BJH analyses. The pores resulting from the solvethermal reaction centralized at 3.7 and 9.5 nm, matching the above result well and the surface area reached 169.79 g/m^2, providing numerous affinity sites to capture endogenous phosphopeptides. The original Fe_3O_4 exhibited a saturation magnetization value of 58.51 emu/g. While after coating with another three shells, the value decreased to 10.76 emu/g. Attributed to subsequent processes of selective etching and calcination, the saturation magnetization value increased to 15.7 emu/g, which would favour the easy separation of YS Fe_3O_4@$mTiO_2$@$mSiO_2$ (Fig. S3, ESI†).

The YS Fe_3O_4@$mTiO_2$@$mSiO_2$ was supposed to efficiently and selectively enrich endogenous phosphopeptides from the complex sample (Scheme 2). At first, the enrichment effect was evaluated with simple samples. Without enrichment the tryptic digests of β-casein showed lots of high-density non-phosphopeptides and the signal of phosphopeptides was suppressed. However, after enrichment with YS Fe_3O_4@$mTiO_2$@$mSiO_2$, three significant peaks corresponding to phosphopeptides were identified. Compared with the commercial TiO_2 (surface area: 61.25 g/m^2, Fig. S8, ESI†), the YS Fe_3O_4@$mTiO_2$@$mSiO_2$ demonstrated the higher enrichment efficacy and selectivity (Fig. 4a-c), which may be a result of the higher surface area and the special yolk-shell structure. Inspired by this, a detection limit experiment was subsequently conducted. The intensity strength of enriched phosphopeptides was positively related to the primitive concentration of tryptic digests of β-casein. And the detection limit could reach as low as 3 fmol, confirming the high enrichment efficacy (Fig. 4c-e). To further identify the high selectivity of YS Fe_3O_4@$mTiO_2$@$mSiO_2$, different amounts of tryptic digests of BSA as the interference were spiked into the determined amount of tryptic digests of β-casein. The direct analysis of the mixture showed no phosphopeptides but numerous non-phosphopeptides. Brightly, after enrichment with YS Fe_3O_4@$mTiO_2$@$mSiO_2$, only phosphopeptides existed. Even if the molar ratio was 1:1000 (β-casein: BSA),

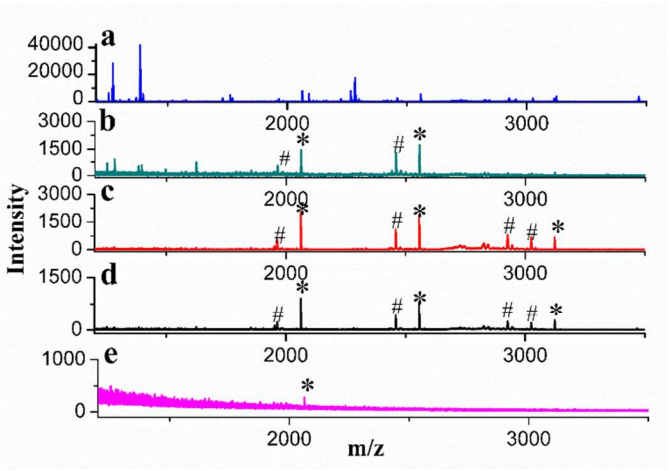

Fig. 4 The MALDI-TOF-MS analysis of tryptic digests of β-casein. (a) Direct analysis; (b) after enrichment with commercial TiO_2; after enrichment with YS Fe_3O_4@$mTiO_2$@$mSiO_2$ when the added amount was (c) 50 fmol, (d) 10 fmol and (e) 3 fmol. * indicates phosphopeptides and # indicates dephosphorylated peptides

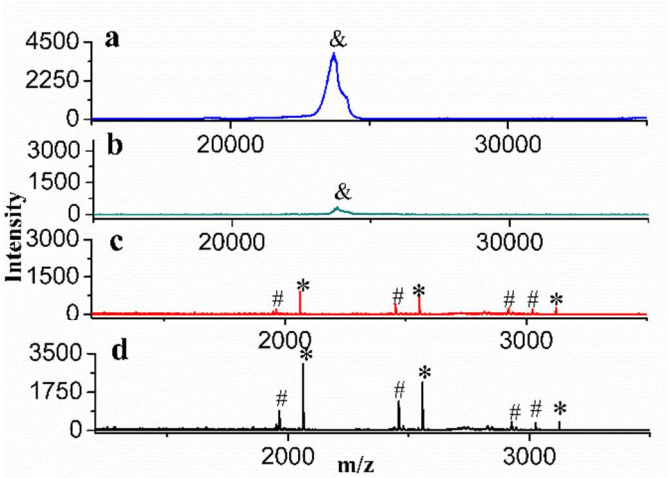

Fig. 5 The MALDI-TOF-MS analysis of the elution after enrichment of a mixture of α-casein protein and tryptic digests of β-casein with (a, c) Fe_3O_4@$mTiO_2$ and (b, d) YS Fe_3O_4@$mTiO_2$@$mSiO_2$.

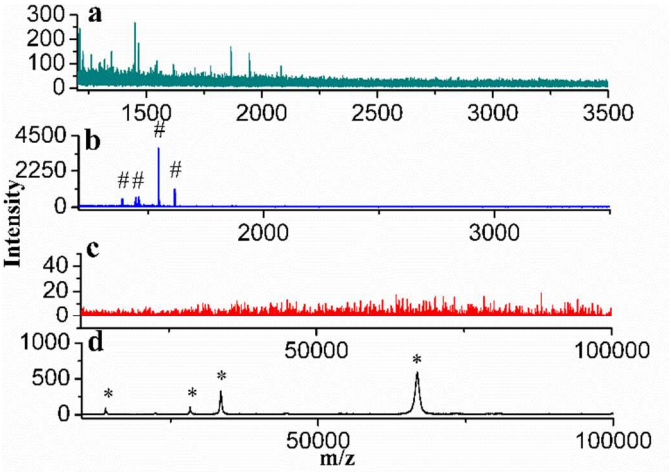

Fig. 6 The MALDI-TOF-MS analysis of human serum. (a) Direct analysis; (b) the endogenous phosphopeptides in the elution, the residual proteins in the (c) elution and (d) supernatant after enrichment with YS Fe_3O_4@$mTiO_2$@$mSiO_2$. # indicates endogenous phosphopeptides and * indicates residual proteins in human serum.

phosphopeptides could still be selectively captured (Fig. S4, ESI†). For YS Fe_3O_4@$mTiO_2$@$mSiO_2$, the outmost $mSiO_2$ shell would act as a size-dependent sieve to exclude the large-molecule proteins out beneficial for efficient and selective enrichment of phosphopeptides. To test this functionality, we applied YS Fe_3O_4@$mTiO_2$@$mSiO_2$ and Fe_3O_4@$mTiO_2$ in parallel for the enrichment of a mixture of α-casein (model phosphoprotein) and tryptic digests of β-casein (a mimic of the complex sample, mass ratio: 100:1). After enrichment, the elution of YS Fe_3O_4@$mTiO_2$@$mSiO_2$ contained very little α-casein with respect to high-abundance α-casein in the elution of Fe_3O_4@$mTiO_2$. On the contrast, as for the case of small-molecule peptides, the situation was opposite (Fig. 5). In detail, although both YS Fe_3O_4@$mTiO_2$@$mSiO_2$ and Fe_3O_4@$mTiO_2$ could capture the phosphopeptides, the signal intensity of phosphopeptides in the elution of Fe_3O_4@$mTiO_2$ was much weaker. It was speculated α-casein would cover and occupy lots of affinity sites on the Fe_3O_4@$mTiO_2$ in view of the large amount, which mostly affected the enrichment efficacy of phosphopeptides. However, the diffusion of large-molecule α-casein (23690 Da, radius of gyration is about 4.5 nm) through the narrow mesopore channels (2.7 nm) distributing within the outmost $mSiO_2$ shell on the YS Fe_3O_4@$mTiO_2$@$mSiO_2$ was relatively difficult, resulting in the size-exclusion effect to improve the enrichment efficacy.

After all, we applied the YS Fe_3O_4@$mTiO_2$@$mSiO_2$ in the selective enrichment of endogenous phosphopeptides from human serum. The direct analysis of human serum showed none of endogenous phosphopeptides, accompanied with lots of high-density endogenous non-phosphopeptides and proteins. However, after enrichment only four endogenous phosphopeptides with high signal-to-noise were detected, which showed better enrichment selectivity and efficacy than previous studies.[8] In the high-molecular range, two obvious proteins (*e.g.* human serum albumin, 67 kDa, 5*7*7 nm) were found out in the supernatant with respect to nothing in the elution, all of which hinted the effective capacity of YS Fe_3O_4@$mTiO_2$@$mSiO_2$ for selective enrichment of endogenous phosphopeptides from the complex sample (Fig. 6).

In summary, a novel magnetic yolk-shell Fe_3O_4@$mTiO_2$@$mSiO_2$ nanocomposite was successfully developed. The nanocomposite exhibited a strong magnetic response, high enrichment selectivity and efficacy towards phosphopeptides and the size-exclusion effect, which was suitable for selective enrichment of endogenous phosphopeptides from the complex sample. With all these advances, it is believed the nanocomposite would be applied in many other fields in the future.

This work was supported by the China State Key Basic Research Program Grant (2013CB911202, 2012CB910604), the Creative Research Group Project of NSFC (21321064), the National Natural Science Foundation of China (21235006, 81161120540), National Key Special Program on Infection diseases (2012ZX10002009-011), Analytical Method Innovation Program of MOST (2012IM030900) to H. F. Zou.

Notes and references

[a] Shanghai Key Laboratory of Functional Materials Chemistry, East China University of Science and Technology, Shanghai 200237, China. E-mail: weibingzhang@ecust.edu.cn

[b] CAS Key Laboratory of Separation Sciences for Analytical Chemistry, National Chromatographic R&A Center, Dalian Institute of Chemical Physics, Chinese Academy of Sciences (CAS), Dalian 116023, China; E-mail: hanfazou@dicp.ac.cn.

†Electronic Supplementary Information (ESI) available: experimental details and additional figures. See DOI: 10.1039/c000000x/

1 (a) G. Cheng, Y. Wang, Z. Wang, X. Sui, J. Zhang and J. Ni, *RSC Adv.*, 2014, **4**, 7694-7702; (b) L. Zhao, H. Qin, Z. Hu, Y. Zhang, R. a. Wu and H. Zou, *Chem. Sci.*, 2012, **3**, 2828; (c) Y. Yan, Z. Zheng, C. Deng, Y. Li, X. Zhang and P. Yang, *Anal. Chem.*, 2013, **85**, 8483-8487; (d) J. C. Smith, M. A. Duchesne, P. Tozzi, M. Ethier and D. Figeys, *J. Proteome. Res.*, 2007, **6**, 3174-3186.

2 (a) Y. Yan, X. Sun, C. Deng, Y. Li and X. Zhang, *Anal. Chem.*, 2014, **86**, 4327-4332; (b) Y. Liang, X. He, L. Chen and Y. Zhang, *RSC Adv.*, 2014, **4**, 18132-18135; (c) W. F. Ma, Y. Zhang, L. L. Li, L. J. You, P. Zhang, Y. T. Zhang, J. M. Li, M. Yu, J. Guo, H. J. Lu and C. C. Wang, *ACS Nano*, 2012, **6**, 3179-3188; (d) T. E. Thingholm, T. J. Jorgensen, O. N. Jensen and M. R. Larsen, *Nat. Protoc.*, 2006, **1**, 1929-1935; (e) Y. Li, X. M. Zhang and C. H. Deng, *Chem. Soc. Rev.*, 2013, **42**, 8517-8539; (f) W. F. Ma, Y. T. Zhang, M. Yu, J. X. Wan and C. C. Wang, *RSC Adv.*, 2014, **4**, 9148–9151.

3 (a) Z. Lu, M. Ye, N. Li, W. Zhong and Y. Yin, *Angew. Chem. Int. Ed.*, 2010, **49**, 1862-1866; (b) G. Cheng, Z. G. Wang, Y. L. Liu, J. L. Zhang, D. H. Sun and J. Z. Ni, *ACS Appl. Mater. Interfaces*, 2013, **5**, 3182-3190; (c) Y. Zhang, W. F. Ma, C. Zhang, C. C. Wang and H. J. Lu, *ACS Appl. Mater. Interfaces*, 2014, **6**, 6290-6299.

4 (a) R. Tian, H. Zhang, M. Ye, X. Jiang, L. Hu, X. Li, X. Bao and H. Zou, *Angew. Chem. Int. Ed.*, 2007, **46**, 962-965; (b) A. Bouamrani, Y. Hu, E. Tasciotti, L. Li, C. Chiappini, X. Liu and M. Ferrari, *Proteomics*, 2010, **10**, 496-505; (c) Y. Hu, A. Bouamrani, E. Tasciotti, L. Li, X. W. Liu and M. Ferrari, ACS Nano, 2010, **1**, 439-451; (d) Z. Y. Gu, Y. J. Chen, J. Q. Jiang and X. P. Yan, *Chem. Commun.*, 2011, **47**, 4787-4789; (e) N. R. Sun, C. H. Deng, Y. Li and X. M. Zhang, *ACS Appl. Mater. Interfaces*, 2014, **6**, 11799–11804.

5 (a) H. Wan, H. Qin, Z. Xiong, W. Zhang and H. Zou, *Nanoscale*, 2013, **5**, 10936-10944; (b) W. Zhao, H. Chen, Y. Li, L. Li, M. Lang and J. Shi, *Adv. Fun. Mater.*, 2008, **18**, 2780-2788; (c) Y. Chen, H. R. Chen, L. M. Guo, Q. J. He, F. Chen, J. Zhou, J. W. Feng and J. L. Shi, *ACS Nano*, 2010, **1**, 529-539.

6 (a) X. Fang, C. Chen, Z. Liu, P. Liu and N. Zheng, *Nanoscale*, 2011, **3**, 1632-1639; (b) Y. Fang, G. Zheng, J. Yang, H. Tang, Y. Zhang, B. Kong, Y. Lv, C. Xu, A. M. Asiri, J. Zi, F. Zhang and D. Zhao, *Angew. Chem. Int. Ed.*, 2014, **53**, 5366-5370; (c) J. Yang, D. Shen, L. Zhou, W. Li, J. Fan, A. M. El-Toni, W. X. Zhang, F. Zhang and D. Zhao, *Adv. Health. Mater.*, 2014.

7 (a) Y. Yang, X. Liu, X. Li, J. Zhao, S. Bai, J. Liu and Q. Yang, *Angew. Chem. Int. Ed.*, 2012, **51**, 9164-9168; (b) H. Wan, Y. Zhang, Z. Y. Liu, G. J. Xu, G. Huang, Y. S. Ji, Z. C. Xiong, Q. Q. Zhang, J. Dong, W. B. Zhang and H. F. Zou, *Nanoscale*, 2014, **6**, 8743-8753; (c) Y. Yang, J. Liu, X. Li, X. Liu and Q. Yang, *Chem. Mater.*, 2011, **23**, 3676-3684.

8 (a) G. Cheng, X. Yu, M. D. Zhou and S. Y. Zheng, *J. Mater. Chem. B*, 2014, **2**, 4711–4719; (b) Z. Lu, J. C. Duan, L. He, Y. X. Hu and Y. D. Yin, *Anal. Chem*., 2010, **82**, 7249–7258; (c) Z. G. Wang, G. Cheng, Y. L. Liu, J. L. Zhang, D. H. Sun and J. Z. Ni, *J. Mater. Chem. B*, 2013, **1**, 1491-1500.

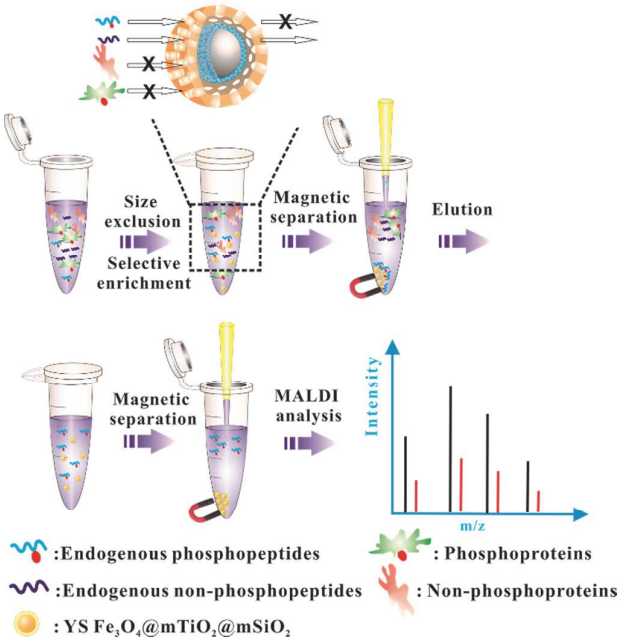

With advances of the strong magnetic response, improved diffusion of peptides, numerous affinity sites towards phosphopeptides and the size-exclusion effect, a novel magnetic yolk-shell Fe_3O_4@mTiO_2@mSiO_2 nanocomposite could efficiently and selectively enrich endogenous phosphopeptides from the complex sample.